EACS 2016 – 6th European Conference on Structural Control Sheffield, England: 11-13 July 2016
Paper No. 151

PERFORMANCE ASSESSMENT OF A NOVEL ENERGY HARVESTING-ENABLED TUNED MASS-DAMPER-INERTER (EH-TMDI) FOR WHITE NOISE-EXCITED STRUCTURES

Salvi, J.*, Giaralis, A.

Department of Civil Engineering, City University of London
Northampton Square, London EC1V 0HB, UK

*Corresponding Author: jonathan.salvi@city.ac.uk

ABSTRACT. In this paper the potential of a novel dynamic vibration absorber termed energy harvesting-enabled tuned mass-damper-inerter (EH-TMDI) is assessed for simultaneous vibration suppression and power generation in white-noise force- and base acceleration-excited structures modelled as damped single-degree-of-freedom (SDOF) oscillators. The considered EH-TMDI comprises a classical linear TMD incorporating an electromagnetic energy harvester connected in series with an inerter device to link the attached TMD mass to the ground in a sky-hook configuration. Pertinent frequency response functions are analytically derived from the underlying equations of motion of EH-TMDI-equipped SDOF primary structures as functions of a number of dimensionless parameters associated with the mechanical properties of the EH-TMDI device and the primary structure. It is shown through appropriate parametric analyses that by varying the mass amplification constant of the inerter device and by adjusting stiffness and damping properties of the TMD using standard optimum TMD design formulae, enhanced vibration suppression (in terms of deflection variance of the primary structure) *and* energy harvesting (in terms of relative velocity variance at the terminals of the harvester) may be achieved *simultaneously* for a fixed attached TMD mass. Overall, the herein reported analytical data and parametric analysis point to the fact that the EH-TMDI is amenable to a meaningful multi-objective optimum design, which may simultaneously minimise the primary structure oscillations and maximise power generation.

KEYWORDS: Tuned Mass Damper, Inerter, Energy Harvesting, White-Noise Excitation.

1 INTRODUCTION

The tuned mass-damper (TMD) is arguably the most widely considered dynamic vibration absorber for passive vibration control of mechanical and civil engineering structures and of structural components subject to various different types of excitations, including random broadband vibrations [1–8].

The TMD comprises a free-to-vibrate mass attached to a host (primary) structure through a linear spring in parallel with a dashpot (e.g., a linear viscous damper). The coefficients are appropriately tuned for an *a-priori* given attached mass and primary structure, such that a resonant out-of-phase motion (compared to that of the primary structure) of the attached mass is achieved. In this manner, significant kinetic energy is transferred from the primary structure to the attached mass, and eventually dissipated by the dashpot in the form of heat.

Over the past decade, the potential of the TMD to transform kinetic energy into electricity from large-amplitude low-frequency oscillating primary structures has been investigated in different studies [9–15]. This is achieved by replacing (or complementing) the dashpot of the TMD with either electromagnetic devices, for large-scale applications (e.g. [9–13, 15]), or piezoelectric materials, for small-scale applications (e.g. [12, 14]), for the case of narrowband dynamic excitations, which can be modelled as harmonic or sinusoidal functions.

Pertinent theoretical and experimental work [13–15] established that vibration suppression and energy harvesting using passive TMDs are conflicting objectives, independently of the scale of the application or the adopted energy harvesting technology. However, the problem of simultaneous vibration suppression and energy harvesting from linear passive TMD-equipped primary structures subject to broadband dynamic excitations modelled as Gaussian white noise received much less attention in the literature. Indeed, most of the research studies assuming broadband or white-noise excitations focus solely on the energy harvesting performance and, with very few exceptions (see e.g. [11]), they concern small-scale applications using piezoelectric materials for kinetic-to-electric energy conversion (see e.g. [16, 17] and references therein).

To this end, this paper explores the potential of a novel passive dynamic vibration absorber termed energy harvesting-enabled tuned mass-damper-inerter (EH-TMDI), for simultaneous vibration suppression and energy harvesting, in white noise-excited primary structures modelled as single-degree-of-freedom (SDOF) oscillators. The considered EH-TMDI couples the classical TMD with: (a) an electromagnetic motor (EM), which functions as an energy harvester, connected in series with (b) an inerter device [18], in a sky-hook configuration. In this regard, the apparent inertia of the TMD and the relative velocity between the terminals of the EM depend on the properties of the grounded inerter.

The latter is a linear two-terminal device of negligible mass, originally defined by Smith [18], which resists the relative acceleration of its terminals by a constant of proportionality, called inertance, having mass units and being independent from the physical device mass. In this re-

spect, the EH-TMDI shares some similarity with dual-mass TMDs considered in the literature to achieve enhanced energy harvesting capabilities through dynamic mass amplification using EM devices [19] or piezoelectric material [20]. However, in the EH-TMDI the mass amplification effect comes from a grounded inerter, which does not add any significant weight to the overall dynamical system.

The remaining of the paper is organised as follows. In Section 2 the topology of the EH-TMDI for SDOF primary structure is described and the underlying dimensionless mechanical parameters that fully state the dynamic behaviour of the overall structural system are defined. In Section 3, the equations of motion of the considered system are derived in the time domain, and the analytical frequency response functions are reported. Section 4 furnishes analytical results from a parametric study of white-noise force- and base-excited EH-TMDI-equipped SDOF structures pertaining to the achieved level of vibration suppression and to the available energy to be harvested. Focus is placed on the trade-off between vibration suppression and energy harvesting achieved by the proposed configuration. Lastly, Section 5 summarises the main conclusions.

2 DESCRIPTION OF THE PROPOSED EH-TMDI CONFIGURATION

Consider the class of structural systems amenable to be modelled as linear damped SDOF oscillators characterised by the natural frequency ω_s and the damping ratio ζ_s defined by:

$$\omega_s = \sqrt{\frac{k_s}{m_s}}, \quad \zeta_s = \frac{c_s}{2\sqrt{k_s m_s}}, \tag{1}$$

where m_s, k_s, and c_s are the mass, stiffness, and damping coefficients of the SDOF oscillator, respectively. The classical linear TMD aims to suppress the oscillations of such structures due to dynamic force or base excitations by attaching a mass m_T via a linear dashpot with damping coefficient c_T and a linear spring of stiffness k_T as shown in Fig. 1a.

Introduced by Marian and Giaralis [21], the tuned mass-damper-inerter (TMDI) improves the vibration suppression capabilities of the classical TMD by incorporating an inerter device to link the attached TMD mass to the ground in a sky-hook configuration as shown in Fig. 1b. This is achieved by exploiting the mass amplification attribute of the grounded inerter, without adding any significant weight to the overall structural system.

To elaborate further on this point, note that the ideal inerter, as conceptually defined by Smith [18], is a linear two-terminal device of negligible physical mass developing an internal (resisting) force $F_I(t)$ proportional to the relative acceleration of its terminals, as shown in the inlet of Fig. 1b:

$$F_I(t) = b\left(\ddot{x}_2(t) - \ddot{x}_1(t)\right), \tag{2}$$

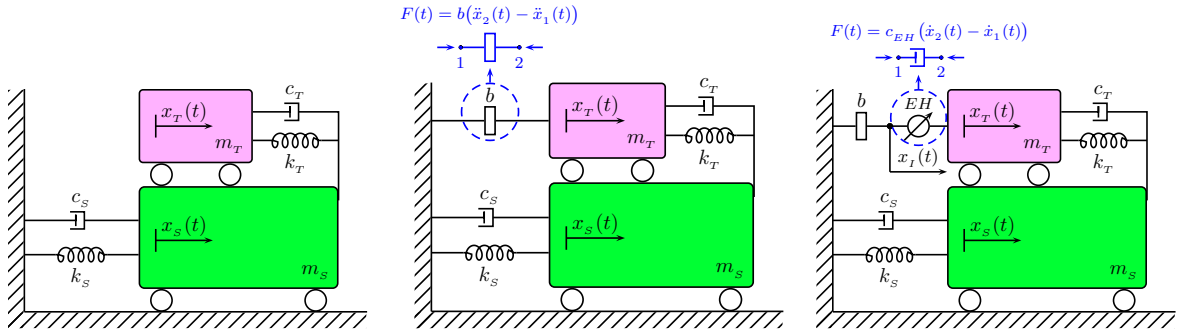

(a) TMD. (b) TMDI. (c) EH-TMDI.

Figure 1: Structural parameters and absolute (relative to the ground) dynamic degrees of freedom of a structural system composed of a SDOF primary structure (subscript S) equipped with different devices, within a sky-hook layout (subscripts T, I, label EH).

where $x_1(t)$, $x_2(t)$ are the displacement coordinates of the inerter terminals and, hereafter, a dot over a symbol signifies differentiation with respect to time t. The constant of proportionality b is the so-called inertance, which has mass units and fully characterises the behaviour of an ideal inerter. In light of Eq. (2), and by considering massless inerter, TMD spring and damper, notice that for an excited SDOF primary structure the TMDI with inertance b and attached mass m_T coincides with the classical TMD with attached mass $m_T + b$. In this respect, the TMDI natural frequency ω_T and damping ratio ζ_T are defined as [22]:

$$\omega_T = \sqrt{\frac{k_T}{m_T + b}}, \quad \zeta_T = \frac{c_T}{2\sqrt{k_T(m_T + b)}}. \tag{3}$$

Herein, the energy harvesting-enabled tuned mass-damper-inerter (EH-TMDI) configuration shown in Fig. 1c is considered, aiming at simultaneous vibration suppression and energy scavenging from SDOF primary structures subject to random excitation. Specifically, the EH-TMDI incorporates a standard linear electromagnetic motor (EM), similar to those considered in the literature for energy harvesting from large-amplitude low-frequency oscillations [12, 13, 15, 23, 24], connected in series with the grounded inerter and the attached mass of the TMDI. The EM contributes a force proportional to the relative velocity of its two terminals to the overall structural system in Fig. 1c and, therefore, can be modelled as a dashpot with viscous damping coefficient c_{EH} as shown in the inlet of Fig. 1c [13, 24].

In this work, the EM damping coefficient is taken as constant during the excitation (i.e., shunt damping in passive operation mode) [13]. This assumption implies that the EM is not

harvesting energy as is connected to a purely resistant circuit, whereas an energy harvesting circuit would result in a time-varying EM damping coefficient (see e.g. [15]). Still, the above assumption is sufficient for the purposes of the parametric study in Section 4, which aims to evaluate the changes to the vibration suppression performance and to the available energy to be harvested by the EM for different mechanical properties of the devices comprising the EH-TMDI configuration in Fig. 1c, rather than to quantify the actual amount of energy harvested by the EM. The latter requires the specification of a particular EM, energy harvesting circuitry, and energy storage or usage such that a detailed modelling of the underlying coupled electromechanical equations can be achieved (see e.g. [13,15]). However, such considerations fall outside the scope of this work. To this end, the damping ratio ζ_{EH} associated with the EM is defined as:

$$\zeta_{EH} = \frac{c_{EH}}{2\sqrt{k_T(m_T + b)}}, \tag{4}$$

in analogy to the definitions in Eq. (3), by accounting an effective harvesting damping ratio $\zeta_{EH,h}$ and a parasitic (mechanical) damping ratio $\zeta_{EH,p}$, that is, $\zeta_{EH} = \zeta_{EH,h} + \zeta_{EH,p}$.

As a closure to this section, notice that several topologies involving different connectivity between the inerter, the EM, and the TMD spring and damper have been examined. The configuration of the EH-TMDI in Fig. 1c is the preferable one since it does not necessarily lead to a trade-off between vibration suppression and energy harvesting as higher values of inertance are assumed within a practical range of interest. This issue is discussed in detail in Section 4, in view of analytical data from a pertinent comprehensive parametric analysis.

3 EQUATIONS OF MOTION FOR RANDOMLY-EXCITED EH-TMDI

The equations of motion for the structural system of Fig. 1c (SDOF primary structure + EH-TMDI) subject to random excitation read as:

$$\begin{cases} m_S\ddot{x}_S(t) + c_S\dot{x}_S(t) + c_T(\dot{x}_S(t) - \dot{x}_T(t)) + k_S x_S(t) + k_T(x_S(t) - x_T(t)) = F_S(t) \\ m_T\ddot{x}_T(t) + c_T(\dot{x}_T(t) - \dot{x}_S(t)) + k_T(x_T(t) - x_S(t)) + c_{EH}(\dot{x}_T(t) - \dot{x}_I(t)) = F_T(t) \\ c_{EH}(\dot{x}_I(t) - \dot{x}_T(t)) + b\ddot{x}_I(t) = 0 \end{cases}, \tag{5}$$

where $x_S(t)$, $x_T(t)$ and $x_I(t)$ are the displacement response processes of the primary structure, of the attached mass, and of the node connecting the inerter to the EM, respectively. Zero-value initial conditions are assumed. In Eq. (5), $F_S(t)$, $F_T(t)$ are the random dynamic forces acting along the degrees of freedom corresponding to the primary structure and to the TMD, respectively. For the case of force-excited primary structures it is taken that $F_T(t) = 0$, whereas for the case of base acceleration-excited primary structures the excitation terms become $F_S(t) = -m_S\ddot{x}_g(t)$ and $F_T(t) = -m_T\ddot{x}_g(t)$, where $\ddot{x}_g(t)$ is the ground acceleration process.

By introducing the following dimensionless parameters, namely the mass ratio μ, the frequency ratio f and the inertance ratio β:

$$\mu = \frac{m_T}{m_S}, \quad f = \frac{\omega_T}{\omega_S}, \quad \beta = \frac{b}{m_S}, \tag{6}$$

and by dividing by $(m_S \omega_S^2) = k_S$, the system of Eq. (5) is written in matrix form as:

$$\mathbf{M}\ddot{\mathbf{x}}(t) + \mathbf{C}\dot{\mathbf{x}}(t) + \mathbf{K}\mathbf{x}(t) = \mathbf{F}(t), \tag{7}$$

where the **M**, **C** and **K** matrices are given as:

$$\begin{aligned}
\mathbf{M} &= \begin{bmatrix} 1 & 0 & 0 \\ 0 & \mu & 0 \\ 0 & 0 & \beta \end{bmatrix} \\
\mathbf{C} &= \begin{bmatrix} 2\zeta_S\omega_S + 2\zeta_T\omega_T(\mu+\beta) & -2\zeta_T\omega_T(\mu+\beta) & 0 \\ -2\zeta_T\omega_T(\mu+\beta) & 2(\zeta_T+\zeta_{EH})\omega_T(\mu+\beta) & -2\zeta_{EH}\omega_T(\mu+\beta) \\ 0 & -2\zeta_{EH}\omega_T(\mu+\beta) & 2\zeta_{EH}\omega_T(\mu+\beta) \end{bmatrix}. \\
\mathbf{K} &= \begin{bmatrix} \omega_S^2 + \omega_T^2(\mu+\beta) & -\omega_T^2(\mu+\beta) & 0 \\ -\omega_T^2(\mu+\beta) & \omega_T^2(\mu+\beta) & 0 \\ 0 & 0 & 0 \end{bmatrix}
\end{aligned} \tag{8}$$

while $\mathbf{F}(t)$, $\mathbf{x}(t)$, $\dot{\mathbf{x}}(t)$, $\ddot{\mathbf{x}}(t)$ are the excitation, displacement, velocity and acceleration process vectors, respectively.

The above system of equations can be conveniently solved in the frequency domain by Fourier transforming Eq. (7) and solving for the vector $\mathbf{X}(ig) = [X_S(ig), X_T(ig), X_I(ig)]^{\mathrm{T}}$, which collects the Fourier-transformed elements of the displacement vector $\mathbf{x}(t)$ written in terms of the normalised frequency $g = \omega/\omega_S$. These operations yield:

$$\mathbf{X}(ig) = \mathbf{H}(ig)\mathbf{F}(ig), \tag{9}$$

where $\mathbf{F}(ig)$ is the excitation vector in the frequency domain, and the receptance matrix $\mathbf{H}(ig)$ is written as:

$$\begin{aligned}
\mathbf{H}(ig) &= [-g^2\mathbf{M} + ig\mathbf{C} + \mathbf{K}]^{-1} = \\
&= \frac{1}{\det(-g^2\mathbf{M} + ig\mathbf{C} + \mathbf{K})} \begin{bmatrix} H_{11}(ig) & H_{12}(ig) & H_{13}(ig) \\ H_{21}(ig) & H_{22}(ig) & H_{23}(ig) \\ H_{31}(ig) & H_{32}(ig) & H_{33}(ig) \end{bmatrix},
\end{aligned} \tag{10}$$

where:

$$
\begin{aligned}
H_{11}(ig) &= [-g^2\mu + ig2(\zeta_T + \zeta_{EH})f(\mu+\beta) + f^2(\mu+\beta)][-g^2\beta + ig2\zeta_{EH}f(\mu+\beta)] + \\
&\quad - [-ig2\zeta_{EH}f(\mu+\beta)]^2 \\
H_{21}(ig) &= (-1)[-ig2\zeta_T f(\mu+\beta) - f^2(\mu+\beta)][-g^2\beta + ig2\zeta_{EH}f(\mu+\beta)] \\
H_{31}(ig) &= [-ig2\zeta_T f(\mu+\beta) - f^2(\mu+\beta)][-ig2\zeta_{EH}f(\mu+\beta)] \\
H_{12}(ig) &= (-1)[-ig2\zeta_T f(\mu+\beta) - f^2(\mu+\beta)][-g^2\beta + ig2\zeta_{EH}f(\mu+\beta)] \\
H_{22}(ig) &= [-g^2 + ig2(\zeta_S + \zeta_T f(\mu+\beta)) + (1 + f^2(\mu+\beta))][-g^2\beta + ig2\zeta_{EH}f(\mu+\beta)], \\
H_{32}(ig) &= (-1)[-g^2 + ig2(\zeta_S + \zeta_T f(\mu+\beta)) + (1 + f^2(\mu+\beta))][-ig2\zeta_{EH}f(\mu+\beta)] \\
H_{13}(ig) &= [-ig2\zeta_T f(\mu+\beta) - f^2(\mu+\beta)][-ig2\zeta_{EH}f(\mu+\beta)] \\
H_{23}(ig) &= (-1)[-g^2 + ig2(\zeta_S + \zeta_T f(\mu+\beta)) + (1 + f^2(\mu+\beta))][-ig2\zeta_{EH}f(\mu+\beta)] \\
H_{33}(ig) &= [-g^2 + ig2(\zeta_S + \zeta_T f(\mu+\beta)) + (1 + f^2(\mu+\beta))][-g^2\mu + \\
&\quad + ig2(\zeta_T + \zeta_{EH})f(\mu+\beta) + f^2(\mu+\beta)] - [-ig2\zeta_T f(\mu+\beta) - f^2(\mu+\beta)]^2
\end{aligned}
\tag{11}
$$

and the superscript -1 denoting matrix inversion.

4 PARAMETRIC STUDY FOR WHITE-NOISE EXCITATION

In this section, a parametric investigation is undertaken to assess the potential of the EH-TMDI in Fig. 1c for simultaneous vibration suppression and energy harvesting in SDOF systems under white-noise force and base acceleration excitations. To this aim, the following dimensionless performance indices are adopted:

$$
\begin{aligned}
I_X &= \frac{\sigma^2_{X_S}}{D} = \int_{-\infty}^{\infty} H_S(ig)\mathrm{d}g\,, \\
I_{EH} &= \zeta_{EH,h}\, f\,(\mu+\beta)\,\frac{\sigma^2_{\dot{X}_T-\dot{X}_I}}{D} = \zeta_{EH,h}\, f\,(\mu+\beta)\,\frac{\sigma^2_{\dot{X}_T} + \sigma^2_{\dot{X}_T} - 2\sigma_{\dot{X}_T\dot{X}_I}}{D} = \\
&= \zeta_{EH,h} f(\mu+\beta)\int_{-\infty}^{\infty} g^2\Big(H_T(ig) + H_I(ig) - 2\sqrt{H_{TI}(ig)H_{IT}(ig)}\Big)\mathrm{d}g\,,
\end{aligned}
\tag{12}
$$

In the above expressions, the index I_X is proportional to the variance of the deflection of the primary structure $\sigma^2_{X_S}$ and is used to quantify the achieved level of vibration suppression by the EH-TMDI, while the index I_{EH} refers to the available energy for harvesting, which is proportional to the variance of the relative velocity occurring at the ends of the harvester $\sigma^2_{\dot{X}_T-\dot{X}_I}$ across all frequencies (see also [11, 16, 17]). For the case of white-noise force-excited primary

structures, the frequency response functions (FRFs) and the denominator D in Eq. (12) read as:

$$\begin{aligned} H_S(ig) &= \left|\frac{H_{11}(ig)}{\Delta}\right|^2, \quad H_T(ig) = \left|\frac{H_{21}(ig)}{\Delta}\right|^2, \quad H_I(ig) = \left|\frac{H_{31}(ig)}{\Delta}\right|^2 \\ H_{TI}(ig) &= \frac{H_{21}(ig)H_{31}(ig)^*}{|\Delta|^2}, \quad H_{IT}(ig) = \frac{H_{31}(ig)H_{21}(ig)^*}{|\Delta|^2}, \quad D = 2\pi\, S_{0,F}\, \omega_S / k_S^2, \end{aligned} \tag{13}$$

where the FRF components are given in Eq. (11), $S_{0,F}$ is the input white-noise power spectrum of constant amplitude across frequencies, * denotes conjugation, and $\Delta = \det(-g^2\mathbf{M} + ig\mathbf{C} + \mathbf{K})$. For the case of primary structures subjected to white-noise base acceleration, the FRFs and the denominator D in Eq. (12) read as:

$$\begin{aligned} H_S(ig) &= \left|\frac{H_{11}(ig)}{\Delta}\right|^2 + \mu\left|\frac{H_{12}(ig)}{\Delta}\right|^2, \quad H_T(ig) = \left|\frac{H_{21}(ig)}{\Delta}\right|^2 + \mu\left|\frac{H_{22}(ig)}{\Delta}\right|^2 \\ H_I(ig) &= \left|\frac{H_{31}(ig)}{\Delta}\right|^2 + \mu\left|\frac{H_{32}(ig)}{\Delta}\right|^2, \quad H_{TI}(ig) = \frac{H_{21}(ig)H_{31}(ig)^*}{|\Delta|^2} + \mu\frac{H_{22}(ig)H_{32}(ig)^*}{|\Delta|^2} \\ H_{IT}(ig) &= \frac{H_{31}(ig)H_{21}(ig)^*}{|\Delta|^2} + \mu\frac{H_{32}(ig)H_{22}(ig)^*}{|\Delta|^2}, \quad D = 2\pi\, S_{0,A}/\omega_S^3 . \end{aligned} \tag{14}$$

In the last equation, all FRFs appearing are defined in Eq. (11), $S_{0,A}$ is the input white-noise acceleration power spectrum of constant amplitude across frequencies (notice that in terms of units $S_{0,A} = S_{0,F}/m_S^2$), and Δ is defined as above.

It is emphasised that the index I_{EH} may significantly overestimate the energy that could be actually harvested in a practical implementation of the EH-TMDI as, despite some recent advancements considering non-linear energy harvesters (see e.g. [25]), such devices operate within a relatively narrow frequency band around resonance conditions, i.e. $g = 1$. However, letting the limits of integration in computing I_{EH} to be (theoretically) unbounded was deemed appropriate in this study as it is consistent with the definition of the index I_X and in alignment with similar indices used in the literature for the purpose at hand [11, 16, 17]. The specification of particular limits around the resonant frequency would involve the consideration of a particular EM device and energy harvesting circuit, which falls beyond the purposes of this investigation aiming to evaluate the change (differences) to the available energy to be harvested by varying the EH-TMDI properties.

The performance indices in Eq. (12) are computed by using standard numerical quadrature rules to evaluate the required integrals. To facilitate studying the performance of the EH-TMDI for simultaneous vibration suppression and energy harvesting as higher values of inertance are considered, the two indices in Eq. (12) are plotted *together* in Figs. 2 and 3 for white-noise force and base-acceleration excitations, respectively. This is done for two different values of

the mass ratio μ (i.e., 1% and 5%), of the structural damping ratio ζ_S (i.e., 2% and 5%), and of the energy harvester damping ratio $\zeta_{EH,h}$ assumed to be constant (i.e., 10% and 20%). In all considered cases, an additional parasitic (mechanical) damping $\zeta_{EH,h} = 1\%$ is considered, in alignment with experimental data reported in the literature [15]. To make possible a comparison between EH-TMDIs with different attached mass, the considered indices are plotted against the inertance-to-mass ratio δ in Figs. 2 and 3, that is (see also [26]),

$$\delta = \frac{\beta}{\mu} = \frac{b}{m_T} \,. \tag{15}$$

To further support a comparison between the two different objectives under study, the values for both indices in Eq. (12) are divided by the peak globally attained value of the indices across all considered values of μ and δ, that is, by $\max_{\delta}\{I_X, I_{EH}\}$. The formulae collected in Table 1 are adopted to determine the natural frequency and damping ratios in Eq. (3) for given mass and inertance ratios. These formulae correspond to optimal tuning parameters for the classical TMD derived in closed-form in [3], for white noise-excited undamped SDOF primary structures in which the TMD mass ratio μ is herein replaced by the sum of the mass ratio plus inertance ratio $\mu + \beta$. In this regard, these expressions do not yield, by any means, optimum design parameters for the EH-TMDI corresponding to any particular optimisation criterion. However, they do yield reasonable values for the stiffness and the damping properties of the EH-TMDI, which suffice for the purposes of this work.

Table 1: Adopted formulae for the computation of the TMDI parameters in Eq. (3) *for different types of loading, as functions of μ and β (for $\beta = 0$, the classical optimum TMD formulae in [3] are retrieved).*

Dynamic loading	f	ζ_T
White-noise force	$\frac{1}{1+\mu+\beta}\sqrt{\frac{2+\mu+\beta}{2}}$	$\sqrt{\frac{(\mu+\beta)(4+3(\mu+\beta))}{8(1+\mu+\beta)(2+\mu+\beta)}}$
White-noise base acceleration	$\frac{1}{1+\mu+\beta}\sqrt{\frac{2-\mu-\beta}{2}}$	$\sqrt{\frac{(\mu+\beta)(4-\mu-\beta)}{8(1+\mu+\beta)(2-\mu-\beta)}}$

Commenting on the plots in Figs. 2 and 3, it is seen that in all considered cases, *simultaneously* improved vibration suppression *and* energy harvesting is achieved for $\delta > 5$ with increasing inertance ratios. For force-excited systems, the rate of improvement decreases as higher inertance values are considered while for base-excited systems, the rate of improvement with increasing inertance is almost linear.

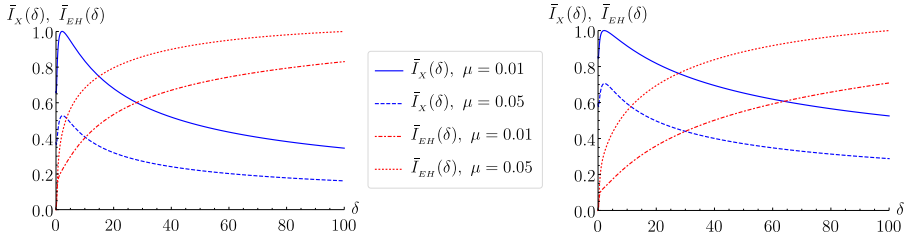

(a) $\zeta_S = 0.02, \zeta_{EH,h} = 0.10$. (b) $\zeta_S = 0.05, \zeta_{EH,h} = 0.10$.

(c) $\zeta_S = 0.02, \zeta_{EH,h} = 0.20$. (d) $\zeta_S = 0.05, \zeta_{EH,h} = 0.20$.

Figure 2: Primary structure dynamic response $\bar{I}_X(\delta)$ and available energy to be harvested $\bar{I}_{EH}(\delta)$ indices, for the case of white-noise force on the primary structure, with $\zeta_{EH,p} = 0.01$.

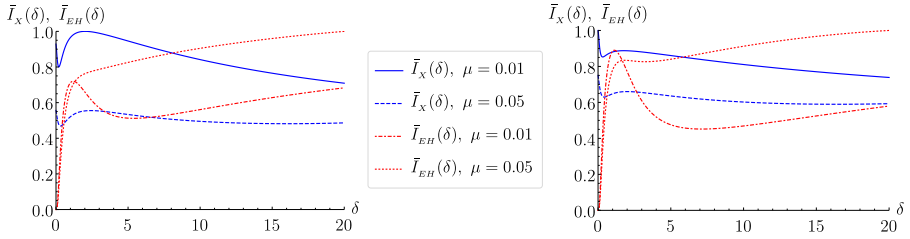

(a) $\zeta_S = 0.02, \zeta_{EH,h} = 0.10$. (b) $\zeta_S = 0.05, \zeta_{EH,h} = 0.10$.

(c) $\zeta_S = 0.02, \zeta_{EH,h} = 0.20$. (d) $\zeta_S = 0.05, \zeta_{EH,h} = 0.20$.

Figure 3: Primary structure dynamic response $\bar{I}_X(\delta)$ and available energy to be harvested $\bar{I}_{EH}(\delta)$ indices, for the case of white-noise base acceleration, with $\zeta_{EH,p} = 0.01$.

In this regard, it is argued that the optimum design of the EH-TMDI does not necessarily involve a trade-off between minimisation of primary structure oscillations and maximisation of power generation, as is the case with the conventional TMD-based energy harvesters found in the literature [13–15]. Moreover, the performance improvement at increasing inertance is more significant for the case of smaller attached mass, that is, the same increase to the inerter value will benefit more the lighter EH-TMDI. This trend is in perfect alignment to what has been reported in the literature [22] for the TMDI in Fig. 2b.

Nevertheless, it is important to note that for base-acceleration excitation, the inertance value should not exceed a certain threshold, beyond which the relative acceleration-proportional force developed within the inerter acts as a destabilising force driving the displacement of the attached mass, and eventually of the primary structure, to excessive amplitudes. This threshold depends on the attached mass but, in all practical cases, is greater than $\beta = 1$. Mathematically, this is manifested through a singular behaviour of the magnitude of the FRFs in Eq. (14). In recognition of this undesirable behaviour, all plots in Fig. 3 are bounded by a threshold value $\delta = 20$.

Turning the attention to the energy harvesting potential of the EH-TMDI, it is seen that for the base-excited primary structures with small attached mass, the available energy to be harvested increases initially and reaches a local maximum with the inertance-to-mass ratio δ, after which it reduces until it reaches a value of δ equal to about 5. The existence of this local maximum depends on both the attached mass ratio and on the damping ratio of the energy harvester. For larger values of $\zeta_{EH,h}$, a less prominent peak is observed (i.e., I_{EH}-δ curves tend to be smoother). Lastly, it is seen that structural damping does influence the shape of the I_{EH}-δ curves in all considered cases, especially for the smaller value of $\zeta_{EH} = 10\%$. This observation suggests that structural damping should not be neglected in quantifying the energy that can be generated by TMD-based energy harvesters, while its value should be estimated as accurately as possible in practical applications.

5 CONCLUDING REMARKS

The potential of a novel dynamic vibration absorber has been assessed for simultaneous vibration suppression and energy harvesting in white noise-excited damped SDOF primary structures, termed energy harvesting-enabled tuned mass-damper-inerter (EH-TMDI).

The EH-TMDI comprises a classical linear TMD, incorporating an electromagnetic energy harvester connected in series with an inerter device to link the attached TMD mass to the ground in a sky-hook configuration.

It has been demonstrated through parametric analyses involving the mechanical properties of the EH-TMDI that, by varying the mass amplification constant of the inerter (inertance) and by adjusting the stiffness and damping properties of the TMD using standard optimum TMD design formulae, enhanced vibration suppression (in terms of deflection variance of the primary

structure) *and* energy harvesting (in terms of relative velocity variance at the terminals of the harvester) may be achieved *simultaneously* for a fixed attached TMD mass. This is not the case with TMD-based energy harvesters commonly considered in the literature, for which a stringent trade-off between vibration suppression and energy harvesting exists.

Furthermore, it has been shown in the considered parametric analyses that the damping of the primary structure appreciably influences the energy harvesting performance of the EH-TMDI. Therefore, the inherent structural damping of primary structures should not be ignored for the sake of facilitating optimum design, and attention should be paid on estimating its value with good accuracy using standard system identification techniques in practical applications.

Overall, the herein reported analytical data and parametric analysis point to the fact that the proposed EH-TMDI is amenable to multi-objective optimum performance-based design. The latter consideration is left for future work, along with accounting for potential deviations from the ideal linear behaviour for the inerter and for the energy harvester.

ACKNOWLEDGEMENTS

This work has been funded by EPSRC in UK, under grant EP/M017621/1. The Authors gratefully acknowledge this financial support.

REFERENCES

[1] Den Hartog JP. *Mechanical Vibrations*, McGraw-Hill, 4th ed., 1956.

[2] Asami T, Nishihara O, Baz AM. Analytical solutions to H_∞ and H_2 optimization of dynamic vibration absorber attached to damped linear systems, *Journal of Vibrations and Acoustics (ASME)*, 124(2):284–295, 2002.

[3] Warburton GB. Optimum absorber parameters for various combinations of response and excitation parameters, *Earthquake Engineering and Structural Dynamics*, 10(3):381–401, 1982.

[4] Salvi J, Rizzi E. Optimum tuning of Tuned Mass Dampers for frame structures under earthquake excitation, *Structural Control and Health Monitoring*, doi: 10.1002/stc.1710, 22(4):707–725, 2015.

[5] Salvi J, Rizzi E, Rustighi E, Ferguson NS. On the optimisation of a hybrid Tuned Mass Damper for impulse loading, *Smart Materials and Structures*, doi:10.1088/0964-1726/24/8/085010, 24(8)(2015)085010, 15 pages, 2015.

[6] Salvi J, Rizzi E. Closed-form optimum tuning formulas for passive Tuned Mass Dampers under benchmark excitations, *Smart Structures and Systems*, doi: 10.12989/sss.2016.17.2.231, 17(2):231–256, 2016.

[7] Bakre SV, Jangid RS. Optimum parameters of tuned mass damper for damped main system, *Structural Control and Health Monitoring*, 14(3):448–470, 2006.

[8] Krenk S, Høgsberg J. Tuned mass absorbers on damped structures under random load, *Probabilistic Engineering Mechanics*, 23(4):408–415, 2008.

[9] Cassidy IL, Scruggs JT, Behrens S, Gavin HP. Design and experimental characterization of an electromagnetic transducer for large-scale vibratory energy harvesting applications, *Journal of Intelligent Material Systems and Structures*, 22(17):2009–2024, 2011.

[10] Tang X, Zuo L. Simultaneous energy harvesting and vibration control of structures with tuned mass dampers, *Journal of Intelligent Materials Systems and Structures*, 23(18):2117–2127, 2012.

[11] Tang X, Zuo L. Vibration energy harvesting from random force and motion excitations, *Smart Materials and Structures*, 21(7)(2012)075025, 9 pages, 2012.

[12] Zuo L, Tang X. Large-scale vibration energy harvesting, *Journal of Intelligent Materials Systems and Structures*, 24(11):1405–1430, 2013.

[13] Gonzalez-Buelga A, Clare LR, Cammarano A, Neild SA, Burrow SG, Inman DJ. An optimised tuned mass damper/harvester device, *Structural Control and Health Monitoring*, 21(8):1154–1169, 2014.

[14] Adhikari S, Ali F. Energy Harvesting Dynamic Vibration Absorbers, *Journal of Applied Mechanics (ASME)*, 80(4):041004-1, 9 pages, 2013.

[15] Zhu S, Shen WA, Xu Y-L. Linear electromagnetic devices for vibration damping and energy harvesting: modeling and testing, *Engineering Structures*, 34:198–212, 2012.

[16] Adhikari S, Friswell MI, Inman DJ. Piezoelectric energy harvesting from broadband random vibrations, *Smart Materials and Structures*, 18(11):115005, 7 pages, 2009.

[17] Li P, Gao S, Cai H. Modeling and analysis of hybrid piezoelectric and electromagnetic energy harvesting from random vibrations, *Microsystem Technologies*, 21(2):401–414, 2015.

[18] Smith MC. Synthesis of Mechanical Networks: the Inerter, *IEEE Transactions on Automatic Control*, 47(10):1648–1662, 2002.

[19] Tang X, Zuo L. Enhanced vibration energy harvesting using dual-mass system, *Journal of Sound and Vibration*, 330(21):5199–5209, 2011.

[20] Aldraihem O, Baz A. Energy Harvester with a Dynamic Magnifier, *Journal of Intelligent Materials Systems and Structures*, 22(6):521–530, 2011.

[21] Marian L, Giaralis A. Optimal design of a novel tuned mass-damper-inerter (TMDI) passive vibration control configuration for stochastically support-excited structural systems, *Probabilistic Engineering Mechanics*, 38:156–164, 2014.

[22] Marian L, Giaralis A. Vibration suppression and energy harvesting in tuned-mass-damper-inerter (TMDI) equipped harmonically support-excited systems, Proceedings of the 6th World Conference on Structural Control and Monitoring, 15–17 July 2014, Barcelona, Spain, 2014.

[23] Scruggs JT, Iwan WD. Control of a Civil Structure Using an Electric Machine with Semiactive Capability, *Journal of Structural Engineering (ASCE)*, 129(7):951–959, 2003.

[24] Palomera-Arias R, Connor JJ, Ochsendorf JA. Feasibility Study of Passive Electromagnetic Damping Systems, *Journal of Structural Engineering (ASCE)*, 134(1):164–170, 2008.

[25] Ooi BL, Gilbert JM, Rashid A, Aziz A. Switching damper for a frequency-tunable electromagnetic energy harvester, *Sensors and Actuators A: Physical*, 234:311–320, 2015.

[26] Hu Y, Chen MZQ. Performance evaluation for inerter-based dynamic vibration absorbers, *International Journal of Mechanical Sciences*, 99:297–307, 2015.